Hindawi
Advances in Civil Engineering
Volume 2019, Article ID 9286819, 12 pages
https://doi.org/10.1155/2019/9286819

Research Article

Analysis of Damage Evolution of Sandstone under Uniaxial Loading and Unloading Conditions Based on Resistivity Characteristics

Guoyin Wu,[1] Kui Wang ,[1,2] Mingjie Zhao,[1,2] Zhichao Nie,[1] and Zhen Huang[1]

[1]*Key Laboratory of Hydraulic and Waterway Engineering of the Ministry of Education, Chongqing Jiaotong University, Chongqing 400074, China*
[2]*Engineering Research Center of Diagnosis Technology and Instruments of Hydro-Construction, Chongqing Jiaotong University, Chongqing 400074, China*

Correspondence should be addressed to Kui Wang; anhuiwk@163.com

Received 12 July 2019; Revised 18 October 2019; Accepted 14 November 2019; Published 7 December 2019

Academic Editor: Eric Lui

In complex rock engineering, understanding the stress state and determining stability and damage evolution are necessary. To more accurately provide a theoretical basis for judging the stress state of bedrock in engineering, this study experimentally addressed the damage evolution of sandstone under loading and unloading conditions. A theoretical relationship between rock resistivity and porosity was obtained according to the Archie formula, which allowed the derivation of the sandstone damage variable expression. Then, sandstone rock samples were used for experimental evaluation, and the feasibility of the theoretically determined damage variable was verified. Finally, through theoretical and experimental comparison analysis, we developed a correlative damage model for sandstone under uniaxial loading and unloading. The results show that the damage variable varies linearly with strain. The proposed correlative equation describes this behavior accurately for loading and unloading conditions. Based on the results of this study, the correlative damage model of sandstone under cyclic loading and unloading conditions can be further improved to be a complete constitutive damage model.

1. Introduction

The damage state of a rock is closely related to engineering construction. It is generally believed that the loads applied to rock masses in geotechnical engineering are mainly compressive stress (loading) states. As excavation of a project progresses, the initial stress state of the rock mass may change, which can cause a change in the rock mass boundary condition and result in stress state redistribution. Subsequently, the newly unloaded rock mass once again experiences loading during construction, resulting in new changes to the existing stress environment. This can, in some cases, lead to failures such as foundation deformation or even collapse. Therefore, for complex rock engineering, understanding the stress state and determining rock mass stability and failure state is necessary.

During the damage process, microcracks inside the rock constantly initiate, propagate, and gradually interconnect to form macrocracks. Studies that only consider conventional mechanical methods are insufficient for determining the failure state of rocks. Recent studies have described the damage state of rock using different methods. Su et al. [1, 2] used uniaxial loading experiments to simulate the failure mode of rock mass and provide some theory reference for the stability control of rock mass in the fault fracture zone. Bagde and Petroš [3, 4] both conducted cyclic uniaxial loading tests on rock samples in rock-prone areas and studied their fatigue and kinetic energy characteristics. This provides a theoretical basis for applications in earthquake studies, rockburst prediction, and control research. Active methods based on elastic waves (ultrasonic waves) and passive methods (acoustic emissions) have also been used.

Through nonlinear ultrasonic testing of damaged concrete, Zhao et al. [5] explored the regularity of the second and third harmonic ratios on multiscale damage. They also obtained the regularity of nonlinear parameters on crack orientation. Liu et al. [6] used ultrasonic technology to investigate the propagation laws of ultrasonic signals through coal material under various loading conditions and obtained the correlation between ultrasonic parameters and stress and strain under cyclic loading conditions. Wang et al. [7] characterized rock damage (microcracks) using integrated ultrasonic and acoustic emission monitoring methods under multistep loading in concrete specimens. They found that the damage evolution not only depended on the stress, but also on the accumulated time. It is known that acoustic wave information is very sensitive to the instantaneous response of rock rupture from these studies, but the data lack regularity in reflecting rock loading from the beginning until rupture is complete. It is thus difficult to fully characterize the damage evolution state of rock. Moreover, during loading and unloading, the water content inside rock fissures has a great influence on rock physical and mechanical properties. The resistivity characteristics of the rock are also extremely sensitive to any pore fluid in fissures. Thus, the rock damage can be described by the change in its electrical properties throughout loading. In the process of loading, damage usually leads to changes in resistivity. In turn, damage is affected by many factors, such as changes in rock porosity, expansion, and penetration of defects (e.g., pores and cracks). By observing changes in rock resistivity, researchers can evaluate the stress state inside the rock and predict the degree of rock damage in order to achieve simple, reliable, undisturbed, nondestructive, and economical results.

The application of electrical resistivity methods to study rock failure processes has achieved results in recent years [8, 9]. As early as the 1960s, Brace and Orange [10] studied changes in resistivity during rock failure and attributed the change to volumetric expansion of the rock and changes in the pore state. Furthermore, Masao et al. [11] observed that the resistivity of dry marble and granite decreased prior to damage under uniaxial compression conditions and then gradually returned to their initial values. Using a method combining mechanical and electrical parameters, Chen and Lin [12] studied the electrical effects of compressive stress on rock and then proposed and verified an equation of state for the rock fracture law. Lü and Sun [13] and Zhang et al. [14] conducted resistivity tests on the damage state of sandstone at different temperatures. The studies showed that resistivity had certain accuracy for rock damage expression. In addition, Kahraman and Yeken [15] found that the uniaxial compressive strength and tensile strength of igneous rock are both linearly related to resistivity. Moreover, Han et al. [16] carried out a laboratory study on the effect of differential pressure on the joint elastic-electrical properties of typical reservoir sandstones. They concluded that joint elastic-electrical properties can reveal subtle rock responses to pressure, which are not discernible when observing elastic or electrical properties alone. Finally, Garcia et al. [17] introduced a new resistivity-based model that quantitatively takes into account actual clay network geometry and the distribution and type of clay minerals present. Nevertheless, most studies have not quantitatively evaluated the degree of rock damage by establishing a damage variable based on resistivity. Specifically, an analytical expression for rock damage based on resistivity has not yet been established, although Wang et al. [18] derived the changing regularity of rock damage variables and resistivity, under loading conditions, based on rock damage theory.

By using the theoretical relationship between resistivity and stress, this study aimed to determine the rock damage variable under uniaxial loading and unloading in order to evaluate the degree of rock damage. This study refers to related theories of elastic mechanics, fracture mechanics, and damage mechanics. Elasticity is a branch of solid mechanics that studies the stress, deformation, and displacement of elastomers due to external forces, boundary constraints, or temperature changes. Substantially, elastic mechanics is the basis of solid mechanics. Fracture mechanics and damage mechanics have been developed based on this as well. The fracture mechanics involved in this study are mainly macroscopic fracture mechanics, which were used to estimate and control the fracture strength by continuous medium mechanical analysis and experiments without involving the internal fracture mechanism of the material. Damage mechanics is used to study the mechanical laws in the process of material or component damage evolution with deformation that eventually leads to damage under various loading conditions. It combines solid physics, material strength theory, and continuum mechanics to study the theory, making up for the shortcomings of fracture mechanics research. In addition, we experimentally verified the effect of the damage variable on the development of sandstone damage with stress and then derived a correlative damage model suitable for describing the uniaxial loading and unloading conditions on the sandstone.

2. Sandstone Damage Variables Based on Resistivity

Establishing the damage variable in this study is based on the Archie formula. It is generally believed that the Archie formula has three restrictions in its use [19]: (1) the experimental object of the Archie formula is a homogeneous sandstone with a porosity of 10–40% and a formation water salinity of 20,000–100,000 mg/L; (2) the effect of rock shale content on electrical conductivity is not considered and the rock skeleton is considered to be an insulator; (3) from the experimental rock properties, the porosity of the rock must be spatially uniform and the saturation of the fluid contained in the rock must be uniform in space, the water contained in the rock cannot be fresh water, and the electrical properties of rock must be isotropic. However, the specific impact of these factors on the formula is not clear. Most of the impact is only a possible factor. From the practical effect, various influencing factors can be eliminated by the change of rock electrical parameters.

2.1. Rock Resistivity Characteristics under Loaded Conditions. According to the formula developed by Archie [20], the resistivity of the rock is expressed as

$$\rho = \left(\frac{ab\rho_w}{\Phi^m}\right)\mathrm{Sr}^{-n}, \tag{1}$$

where a and b are coefficients associated with the rock, ρ_w is the formation water resistivity, Φ is the rock porosity, Sr is the saturation, m is the rock cementation index, which is used to calculate the pore structure of a rock, and n is the rock saturation index, which characterizes the distribution of oil, gas, and water in the pores of the rock. The pore structure of the rock has the greatest influence on m value. The more complex the pore structure, the larger the m value. n is closely related to rock pore shape, and the different water saturation of the rock also has a certain influence on the value of n. In this paper, the coefficient of the Archie formula is obtained by inverting the parameters based on the uniaxial loading and unloading tests' data of multiple samples.

Saturation is defined by

$$\mathrm{Sr} = \frac{V_w}{V_v}, \tag{2}$$

where V_w represents the volume of water in the rock and V_v is the total pore volume in the rock.

For dry rocks, the natural moisture content is small without being saturated. We then assumed that this volume of water did not change during the loading process, defined by porosity, which can be expressed as

$$\mathrm{Sr} = \frac{V_w}{\Phi V}, \tag{3}$$

where V is the total rock volume.

Therefore, the resistivity can be expressed as

$$\rho = \frac{ab\rho_w}{\Phi^m}\left(\frac{V_w}{\Phi}\right)^{-n}. \tag{4}$$

2.2. Analytical Expression of the Damage Variable Based on Resistivity. In order to reduce the influence of coefficients in the Archie formula, the ratio of resistivity to the initial resistivity was used to represent the changing characteristics of rock resistivity. From this, the rock resistivity ratio was obtained:

$$\frac{\rho}{\rho_0} = \left(\frac{\Phi_0}{\Phi}\right)^{m-n}. \tag{5}$$

As long as the porosity of the rock during loading and unloading is known, the corresponding resistivity can be obtained.

In damage mechanics, a damage variable is a measure of the degree of deterioration of a material or structure and is intuitively understood as a percentage of the volume of microcracks or voids in the entire material. Thus, rock damage evolution can be described by the change in porosity. Dai [21] defined the damage variable based on the rock porosity D_φ as

$$D_\varphi = \frac{\Phi_0 - \Phi}{\Phi_0 - \Phi_S}, \tag{6}$$

where Φ_S is the porosity when the rock is destroyed.

In equation (5), the rock resistivity ratio is related to the porosity ratio so that the resistivity can be used instead of the porosity to characterize the development of microcracks, thereby defining the damage variable.

By incorporating equation (5) into equation (6), the damage variable D_ρ defined by the resistivity ratio can be obtained:

$$D_\rho = \frac{1 - (\rho/\rho_0)^{-(1/m-n)}}{1 - (\rho_S/\rho_0)^{-(1/m-n)}}, \tag{7}$$

where ρ_0 is the material's initial resistivity and ρ_S is the resistivity when the material is broken.

Thus, according to equations (5) and (6), we establish a resistivity-based rock damage variable D_ρ by using the porosity as a bridge factor.

3. Experiments on Sandstone Damage under Loading and Unloading Conditions

3.1. Test Principle. Our experimental procedure used stress and strain tests, as well as resistivity tests of sandstone specimens under uniaxial loading and unloading. There are 60 sandstone samples. These sandstone samples were obtained by drilling core samples from representative gray sandstones in Guoyuan Port in Chongqing. Each core sample was turned into cylindrical rock specimens with a diameter (D) of 50 mm and a height (L) of 100 mm and weighing approximately 500 g, and the density is about 2.546 g/cm^2. Throughout the uniaxial loading and unloading tests, the resistivity of the rock was measured continuously.

The quadrupole method of resistivity measurement was used in this experiment. According to the basic principle of the resistivity method, the quadrupole method is powered by a power supply electrode and current passes through the rock sample. The current I flowing between the measuring electrodes and the potential difference ΔU were measured. Then, according to the cross-sectional area S of the rock sample and the length L of the measuring electrode, the resistivity of the rock can be described as

$$\rho = \frac{S}{L}\cdot\frac{\Delta U}{L}. \tag{8}$$

Since sandstone is a brittle material, the change in porosity is mainly caused by the compression and expansion of internal microcracks. The shape parameters of the rock specimen (i.e., diameter D and height L) change negligibly little, so the change in S and L can be ignored when calculating the resistivity.

3.2. Test Process. We used a RMT-150C rock mechanics tester (manufacturer and country of instrument: Wuhan Institute of Rock and Soil Mechanics, Chinese Academy of Sciences, China) as the test loading device. A DUK-2B high-density electrical instrument (manufacturer and country of instrument: China National Group, Chongqing Geological Instrument Factory, China) was used as the electrical test instrument.

The test procedure was as follows.

Open RMT-150C rock mechanic tester and select 1000 kN class pressure head for vertical hydraulic cylinder; place rock specimens, and in order to better measure the resistivity of the test piece, place copper blocks on both ends of the test piece as a good conductor. At the same time, to eliminate the influence of the test device on the resistivity of the test rock, a plastic film was placed on both ends of the copper block as an insulator.

Connect the DUK-2B high-density electric instrument and then connect the copper piece and the electric instrumented through the wire. According to the principle of the four-pole method, two copper wires were welded to the two ends, and, respectively, connected to the power supply electrodes A and B and the measuring electrodes M and N on the electric instrument.

First, preload so that the pressure head and the test piece were in full contact. The resistivity of each rock sample was measured before loading, and the initial value of the resistivity was recorded. Uniaxial compression grading loading measurements were performed, with an average loading rate of 0.02 kN/s. The resistivity for each load was measured, and the corresponding measured voltage V and the flowing current I were recorded. During the initial loading period, the load was measured by 2~5 kN, the medium-term load interval was measured by 5~10 kN, and the postload interval is measured by 5 kN. The unloading started around 70% of the failure stress. Then, the uniaxial compression grading unloading measurements were carried out, with an average unloading rate of 0.01 kN/s. The grading measurement method during the unloading process is the opposite of the loading process. The unloading process continued for approximately 5% of the near-destructive stress and then was reloaded. The reloading process was performed uniaxially, and the measurement process was the same as the initial loading process. The reloading process continued until the rock broke.

A schematic diagram of the test system used for determining the resistivity of the loaded rock is shown in Figure 1.

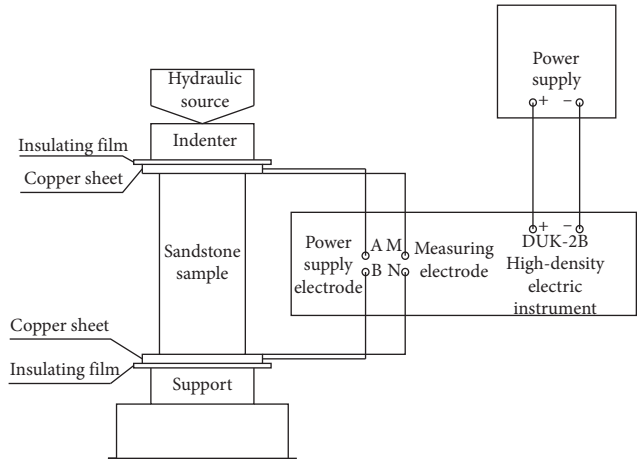

Figure 1: Schematic diagram of the system used to measure the test sample resistivity while loaded.

3.3. Test Results and Analysis

3.3.1. Stress-Strain Curve of the Rock Sample. From a set of loading and unloading tests conducted on each sandstone sample, we present the most representative data in Table 1 and the stress-strain curves of the corresponding samples in Figure 2.

3.3.2. Rock Resistivity-Stress Curve. The voltage (V) and current value (I) under each load were recorded using the DUK-2B high-density electrical instrument. Then, the resistivity value was calculated. The resistivity ratio-stress curve corresponding to the stress-strain curve of sandstone is shown in Figure 3.

3.4. Comparison of the Theoretical Model and Experiments

3.4.1. Theoretical Calculation Curve and Test Curve. In the theoretical relationship, the parameters of the rock need to be determined, including the linear elastic parameters of the rock, the mesostructural parameters of the microfractures, and the coefficients required for the Archie formula. The linear elastic parameters of the rock can be directly obtained from the uniaxial loading test. Based on the uniaxial loading and unloading test data of a number of our sandstone samples, the mesostructural parameters of the microcracks and the coefficients needed for the Archie formula were obtained using parameter inversion, combined with sample mesostructure analyses. The values of these parameters are shown in Table 2.

Once the parameters of the samples were determined, they were substituted into the previously described theoretical relationships. The resistivity ratio was calculated from the data obtained from the tests that were used to create the resistivity ratio-stress test curve. We then calculated the damage variable according to equation (7) and obtained the stress-damage variable test curve. The experimental curves and theoretical fitting curves of the resistivity ratio-stress for sandstone and the experimental curves and theoretical fitting curves of the stress-damage variables are shown in Figures 4 and 5, respectively.

3.4.2. Comparative Analysis of the Resistivity and Damage Variable Test Results and Fitting Curves. From a comparative analysis of experimental curves and theoretical fitting curves, we observed that the values of sandstone resistivity obtained by theoretical calculations and from the experimental tests were in agreement. During loading, the resistivity decreased rapidly in the low stress phase. As the stress increased, the resistivity decreased at a slower rate, while the damage variable increased slowly initially, then rapidly. During the unloading phase, the resistivity increased gradually; however, below the loading curve, the damage variable decreased as the stress decreased and neither returned to its initial value. Finally, during the reloading phase, as the stress increased, the resistivity decreased and the damage variable increased until the rock failed completely. The damage variable established using the resistivity

Table 1: Experimental data on the resistivity of sandstone.

Pressure P (kN)	Stress σ (MPa)	Axial strain ε	Voltage V (mV)	Current A (mA)	Resistivity ρ (Ω·m)	Resistivity ratio ρ/ρ_0
Loading process						
0	0	0	6096.41	0.16	748.14	1.00000
2.00	1.02	0.0007	6096.71	0.20	598.54	0.80004
5.00	2.55	0.0015	6096.41	0.24	498.76	0.66667
10.00	5.09	0.0020	6095.44	0.28	427.44	0.57134
15.00	7.64	0.0022	6095.07	0.31	386.05	0.51602
20.00	10.16	0.0030	6095.20	0.32	373.99	0.49990
30.00	15.28	0.0035	6095.00	0.35	341.92	0.45704
40.00	20.37	0.0039	6094.87	0.38	314.92	0.42095
50.00	25.46	0.0044	6094.88	0.40	299.18	0.39990
60.00	30.56	0.0047	6094.95	0.41	291.89	0.39015
70.00	35.65	0.0051	6094.54	0.42	284.92	0.38084
Unloading process						
70.00	35.65	0.0051	6094.54	0.42	284.92	0.38084
60.00	30.56	0.0051	6094.95	0.42	284.94	0.38086
50.00	25.46	0.0048	6094.40	0.42	284.91	0.38083
40.00	20.37	0.0045	6094.72	0.41	291.88	0.39014
30.00	15.28	0.0042	6094.71	0.40	299.17	0.39989
20.00	10.19	0.0038	6094.65	0.39	306.84	0.41014
15.00	7.64	0.0035	6094.73	0.37	323.43	0.43231
10.00	5.09	0.0032	6094.74	0.34	351.97	0.47046
5.00	2.55	0.0027	6092.77	0.29	412.52	0.55140
Reloading process						
5.00	2.55	0.0027	6092.77	0.29	412.52	0.55140
10.00	5.09	0.0031	6091.80	0.35	341.75	0.45680
15.00	7.64	0.0033	6090.69	0.36	332.20	0.44403
20.00	10.19	0.0035	6091.80	0.38	314.77	0.42073
30.00	15.28	0.0040	6091.56	0.41	291.73	0.38993
40.00	20.37	0.0043	6091.63	0.42	284.78	0.38065
50.00	25.46	0.0046	6091.65	0.45	265.80	0.35528
60.00	30.56	0.0050	6091.70	0.45	265.80	0.35528
70.00	35.65	0.0052	6090.58	0.48	249.14	0.33302
80.00	40.74	0.0055	6090.36	0.49	244.05	0.32621
90.00	45.84	0.0059	6090.17	0.50	239.16	0.31967
100.00	50.93	0.0062	6090.11	0.51	234.47	0.31340
109.72	55.88	0.0066	6090.00	0.51	234.46	0.31339

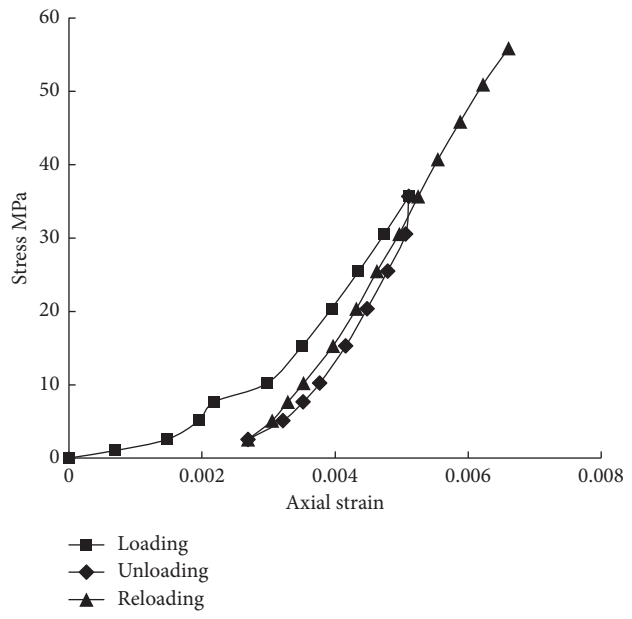

Figure 2: Stress-strain curves of the sandstone sample.

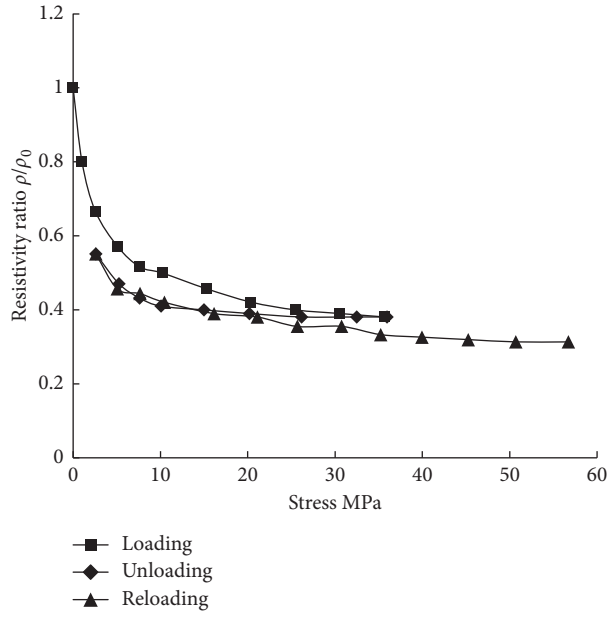

Figure 3: Resistivity-stress curves of the sandstone sample.

Table 2: Selected rock parameters.

Rock type	Elastic modulus E_0 (GPa)	Poisson's ratio v_0	Internal friction angle on the crack surface φ (°)	Rock cementation index m	Rock saturation index n
Sandstone	15.97	0.26	30	2.0	1.33

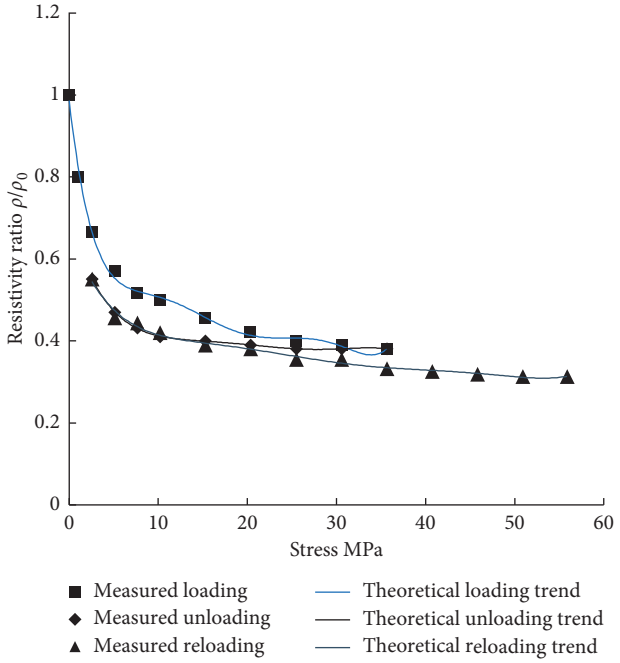

Figure 4: Resistivity-stress experimental curves and theoretical fitting curves for the sandstone samples.

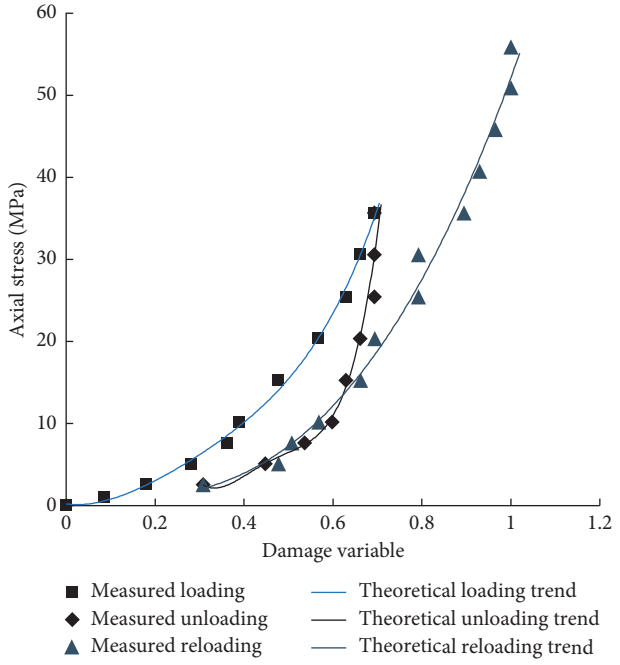

Figure 5: Stress-damage variable experimental curves and theoretical fitting curves for the sandstone samples.

also changed, corresponding to the change in stress. For the resistivity-stress and stress-damage variable curves, there were small errors between the theoretical and experimental curves. However, the laws of resistivity and stress change were more or less consistent during the loading, unloading, and reloading phases. Moreover, we found that when the rock was loaded to 70% of the damage point, the damage variable increased to approximately 0.7, and when it was unloaded to 30%, the damage variable also decreased to approximately 0.3. Therefore, we concluded that the damage variable defined using the resistivity ratio can describe the damage degree of a loaded rock.

4. Correlative Damage Model

4.1. Relationship between Damage Variable and Strain. Regarding a constitutive damage model, the work of Goodman and Boyle [22] assumed that the unloading curve coincides with the reloading curve. Therefore, the constitutive equation for the structural plane should be the same during the unloading and reloading processes, and no redefinition should be required. At present, the axial stress-strain constitutive equations for the rock are empirical equations based on experimental results [23]. Under the premise of the abovementioned assumptions, a nonlinear correlative model for rock damage has been proposed.

During the uniaxial loading and unloading, the volumetric strain of the rock was composed of the volumetric strain ε_V^e of the rock matrix elasticity, the microcrack closed volume strain ε_V^c, and the extended volume strain ε_V^f [24]:

$$\varepsilon_V = \varepsilon_V^e + \varepsilon_V^c + \varepsilon_V^f. \tag{9}$$

Since sandstone is a brittle material, the linear elastic volume strain of the rock matrix is almost negligible during the loading process. The strain occurs mainly due to the closure and expansion of microcracks, so the volumetric strain of sandstone can be expressed as

$$\varepsilon_V = \varepsilon_V^c + \varepsilon_V^f. \tag{10}$$

According to the definition of rock volumetric strain,

$$\varepsilon_V = \frac{\Delta V}{V}. \tag{11}$$

Thus, the total volumetric strain is

$$\varepsilon_V = \frac{\Delta V^e + \Delta V^c + \Delta V^f}{V}, \tag{12}$$

where ΔV represents the total volumetric deformation of the rock, including the volumetric deformation of the rock matrix elasticity ΔV^e, the microcrack closed volume

deformation ΔV^c, and the microcrack extended volume deformation ΔV^f. Among these, the microcrack closed volume strain can be expressed as

$$\varepsilon_V^f = \varepsilon_1^f + 2\varepsilon_2^f. \tag{13}$$

The microcrack extended volumetric strain can be expressed as

$$\varepsilon_V^f = \varepsilon_1^f + 2\varepsilon_2^f, \tag{14}$$

where ε_1^c and ε_2^c are the axial and transverse strain caused by microcrack closure, and ε_1^f and ε_2^f are the axial and transverse strain, respectively, caused by microcrack propagation, respectively.

In any loading state, a change in the porosity of the rock is caused by a closure or expansion of the microfractures; thus, the rock porosity can be expressed as [25]:

$$\begin{aligned}\Phi &= \frac{V_{V0} + \Delta V^c + \Delta V^f}{V} \\ &= \Phi_0 + \frac{\Delta V^c + \Delta V^f}{V} \\ &= \Phi_0 + \varepsilon_V^c + \varepsilon_V^f \\ &= \Phi_0 + \varepsilon_V,\end{aligned} \tag{15}$$

where Φ_0 is the initial porosity of the rock when not loaded.

The sandstone stress-strain and stress-damage curves obtained from our experiments are very similar. Based on expressions (5), (6), (7), and (14), the resistivity ratio can be expressed as follows:

$$D_\rho = \frac{\varepsilon}{\left[\left(\rho_s/\rho_0\right)^{-(1/m-n)} - 1\right]\Phi_0}. \tag{16}$$

Since the rock initial parameter Φ_0, cementation coefficient m, and saturation coefficient n are all fixed values, and the resistivity ratio is also relatively fixed when the rock is destroyed, the linear relationship between the damage variable (D_ρ) and the sandstone strain (ε) is linear. The damage-strain curves obtained by fitting our experimental data to this model are shown in Figure 6.

4.2. Model Building. The damage-strain relationship curve fit shows that the damage-strain relationship in sandstone is linear under both loading and unloading conditions. According to damage mechanics, under conditions of assumed equivalent strain and energy identity, the constitutive rock damage model under uniaxial compression can be expressed as [26]:

$$\sigma = (1 - D)E\varepsilon, \tag{17}$$

where D is the damage variable and E is the initial elastic modulus of sandstone.

This model does not fully describe the rock damage under loading and unloading conditions. In recent years, researchers have proposed structural models for rock properties under cyclic loading conditions from different aspects. Liu et al. [27–29] performed periodic uniaxial compression tests on intermittent joint rock models to study the mechanical fatigue properties of rock under different load parameters. Based on this, a correlative damage model for intermittently jointed rocks under cyclic uniaxial compression was proposed. From the perspective of energy dissipation, Liu et al. [30] proposed the concept of a compaction coefficient to describe the degree of compaction and used a recursive method to establish the correlative damage model under cyclic loading to describe the degree of compactness of rocks.

Notably, during loading and unloading, due to the influence of preloading, the sample was damaged and slight plastic strain was generated. The correction of the elastic modulus to the damage variable is nonlinear during the unloading and reloading phases. Therefore, the sandstone damage characteristics were analyzed based on the above model, and the original model was improved to obtain a correlative model suitable for both loading and unloading. The improved correlative model is as follows:

$$\sigma = \left(r + qD_\rho + pD_\rho^2\right)E\varepsilon, \tag{18}$$

where E is the loading elastic modulus and unloading modulus of sandstone, $E = 15970$ MPa, and p, q, and r are correction factors. The damage variable (D_ρ) is obtained using equation (7).

From our experimental testing, we obtained the stress-strain data for each stage of loading and unloading. The damage variable derived from previous studies was then introduced into the correlative model to obtain a theoretical curve, which is shown in Figure 7.

Considering the fitting results, the correlative model for sandstone damage during loading and unloading was obtained:

Loading phase:

$$\sigma = \left(0.06983 + 0.22911D_\rho + 0.40673D_\rho^2\right)E\varepsilon, \quad 0 \le \varepsilon \le 1. \tag{19a}$$

Unloading phase:

$$\sigma = \left(0.14611 - 0.8767D_\rho + 1.69611\,D_\rho^2\right)E\varepsilon, \quad \varepsilon_1 \le \varepsilon \le \varepsilon_2. \tag{19b}$$

Reloading phase:

$$\sigma = \left(-0.59743 + 1.73672D_\rho - 0.62943D_\rho^2\right)E\varepsilon, \quad \varepsilon_2 \le \varepsilon \le \varepsilon_3. \tag{19c}$$

where ε_1, ε_2, and ε_3 are the loading and unloading nodes.

From Figure 7, we observed that the stress-strain curves obtained from the correlative model presented in this study were essentially consistent with the experimental data and that the stress-strain relationship corresponding to the

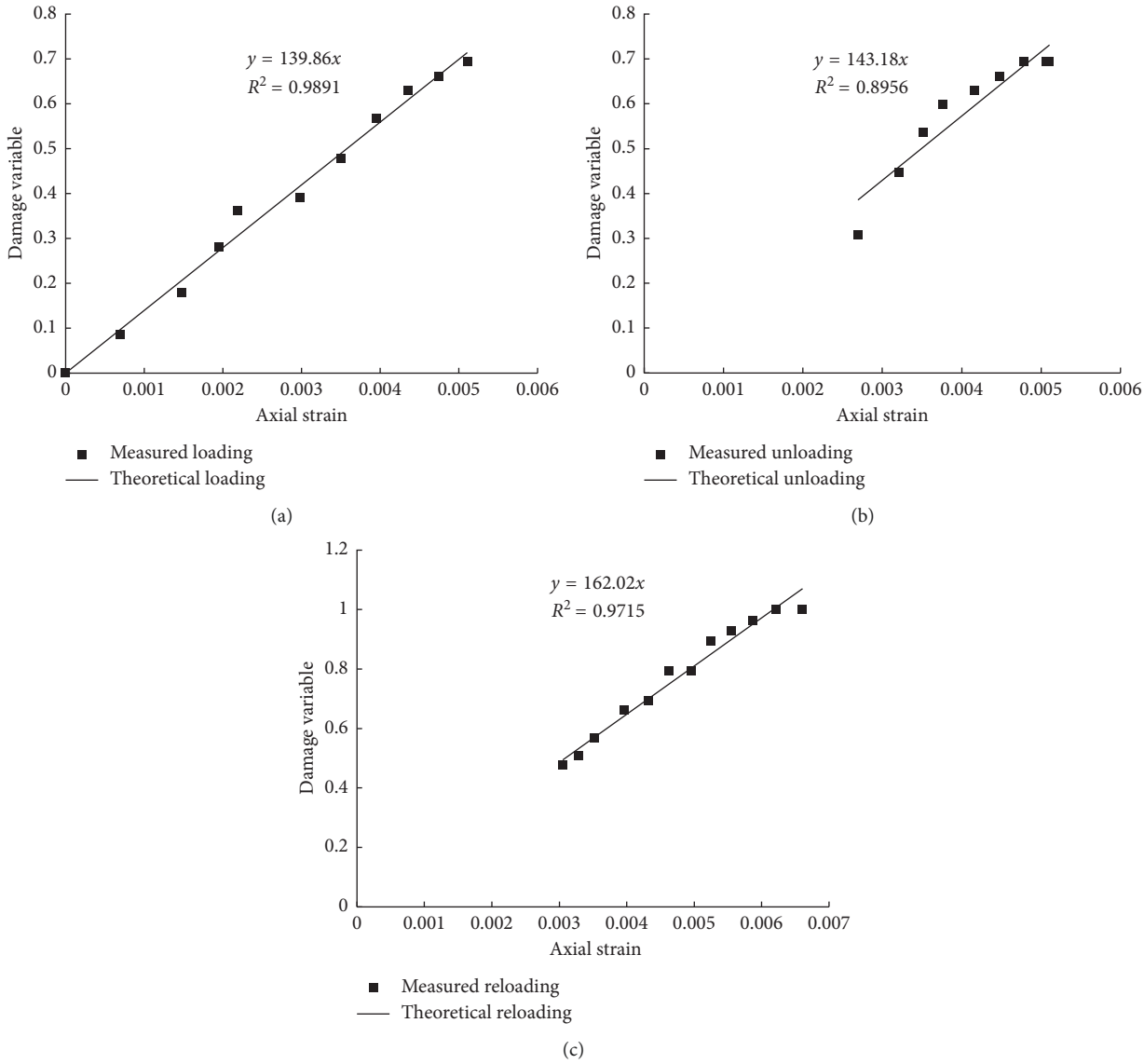

Figure 6: Damage variable-resistivity experimental data and fitted curves. (a) Loading phase. (b) Unloading phase. (c) Reloading phase.

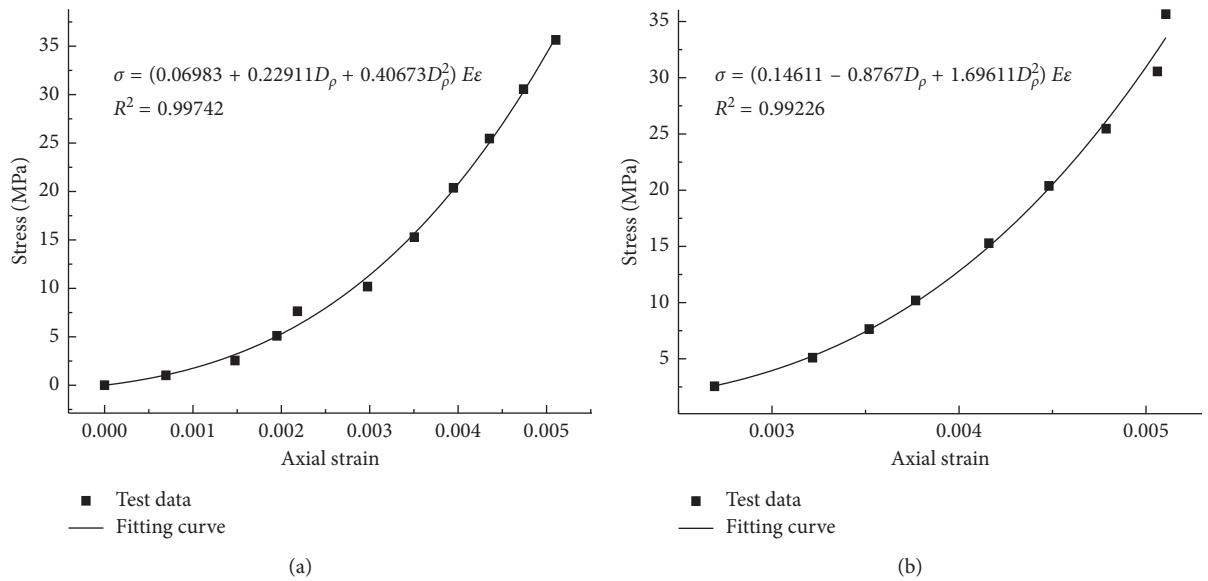

Figure 7: Continued.

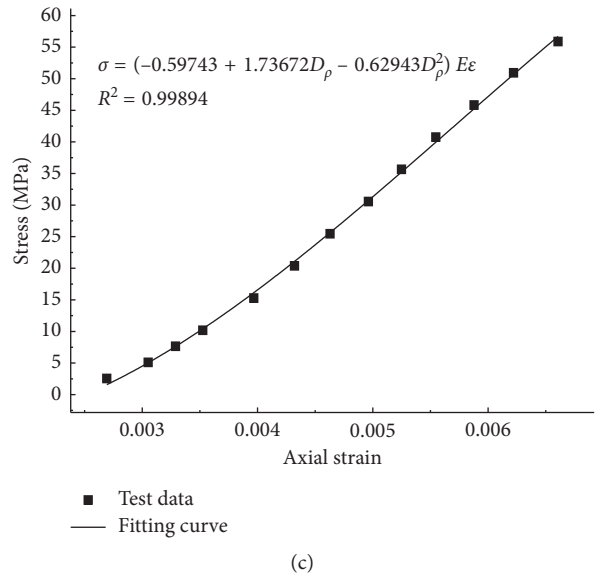

(c)

Figure 7: Sandstone damage correlative model test data and fitted curve. (a) Loading phase. (b) Unloading phase. (c) Reloading phase.

Table 3: Selected rock parameters.

Rock type	Elastic modulus E_0 (GPa)	Poisson's ratio υ_0	Internal friction angle on the crack surface φ (°)	Rock cementation index m	Rock saturation index n
Limestone	21.55	0.257	34	1.98	1.27

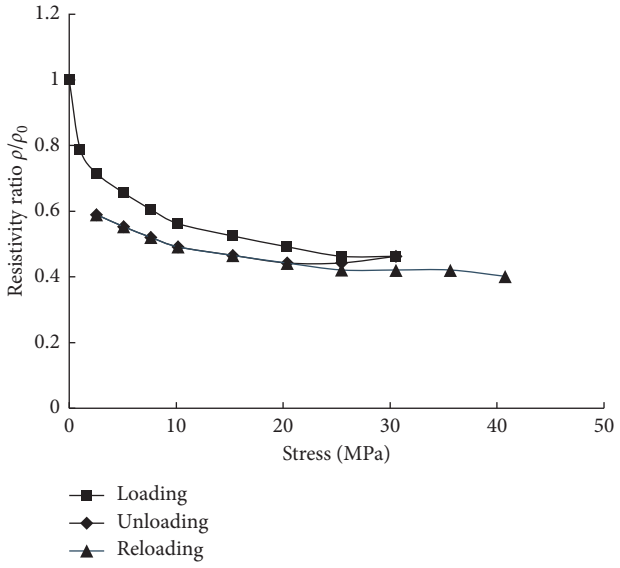

Figure 8: Resistivity-stress test curves of the limestone sample.

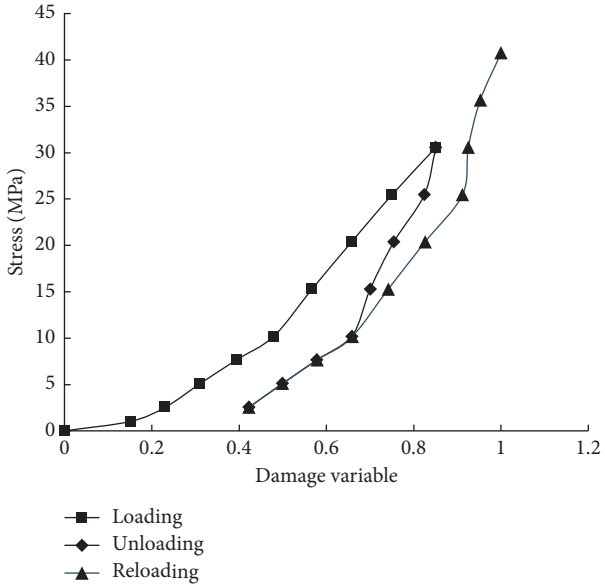

Figure 9: Stress-damage variable test curves of limestone.

upper and lower limits of loading and unloading can be obtained accurately. This demonstrated the feasibility and accuracy of our method.

4.3. Model Verification. The resistivity rock damage correlative model is obtained by fitting the sandstone loading and unloading test data. The correctness of the model type needs to be verified. In view of this, limestone is used as the verification test object. In the uniaxial loading experiment, limestone exhibits the properties of brittle materials, which is similar to the sandstone. Based on the uniaxial loading and unloading test data of a number of our limestone samples, the mesostructural parameters of the microcracks and the coefficients needed for the Archie formula were obtained using parameter inversion, combined with sample mesostructure analyses. The values of these parameters are shown in Table 3.

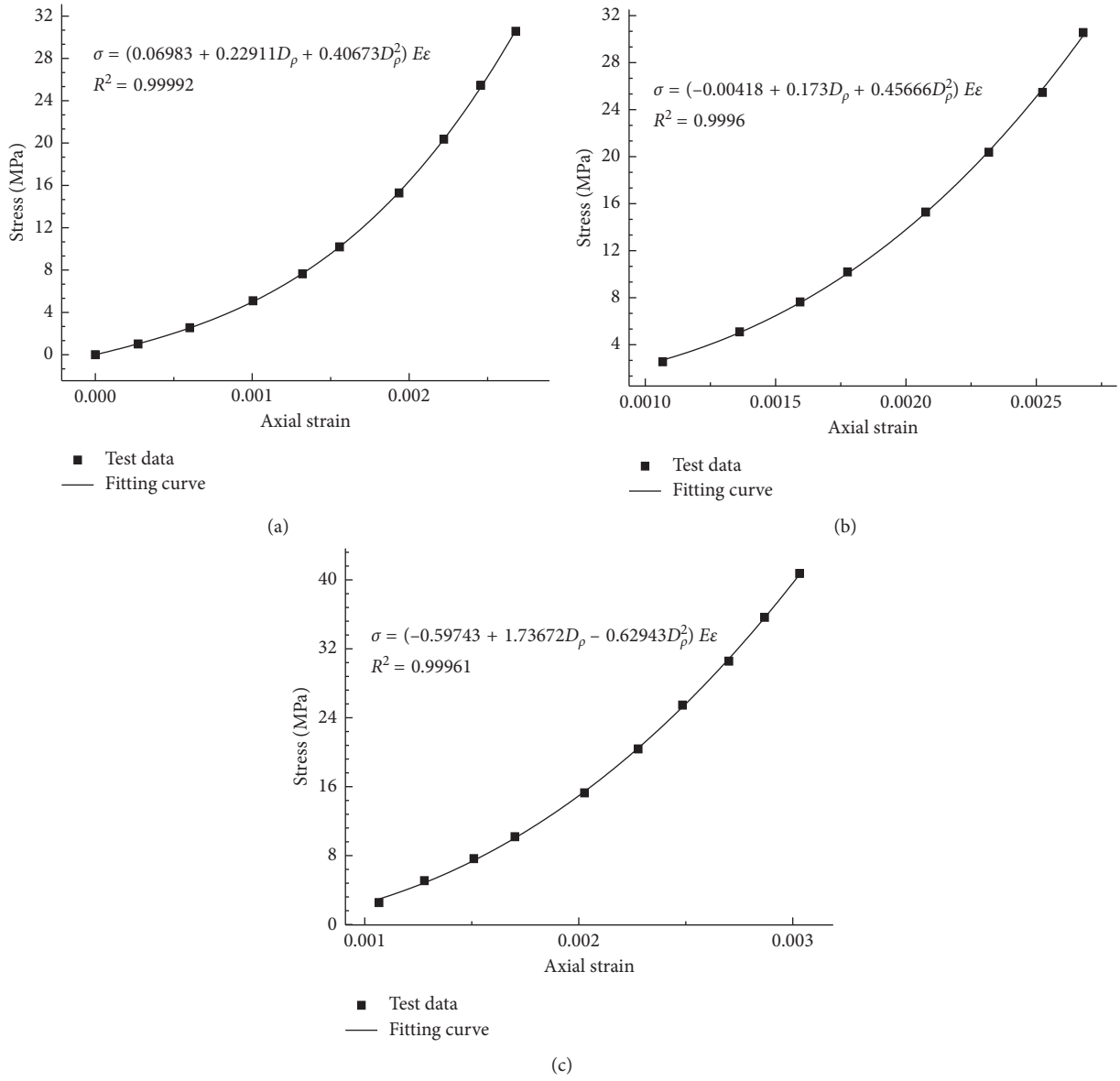

Figure 10: Limestone damage correlative model test data and fitted curve. (a) Loading phase. (b) Unloading phase. (c) Reloading phase.

The operation process of the test verification with limestone is basically the same as that of uniaxial loading and unloading test of sandstone. From the test, the limestone data have been obtained. The resistivity-stress test curve and the stress-damage variable test curve of limestone are shown in Figures 8 and 9.

It can be seen from Figures 8 and 9 that the trend of the damage of limestone varies with the applied stress, which is similar to the sandstone. The phenomenon also shows that the damage variable of brittle rock characterized with the resistivity is reasonable.

Substitute the experimental data of the limestone into the correlative model proposed in this paper, and fit the experimental data to obtain the theoretical stress-strain correlation model curve (Figure 10).

It can be seen from Figure 10 that the data of the verification test is coincident with the correlative model, which also shows the correctness of the damage correlative model proposed in this paper. Moreover, the trend of the stress-strain correlative model during the loading and unloading process is also consistent with the sandstone model. In further research, the model needs to be refined to find the physical meaning of the corrective coefficient in equation (18), which makes the correlative equation become a true constitutive model.

5. Conclusion

Taking into account previous research, this study defines sandstone damage variables based on resistivity in order to describe the degree of rock damage under uniaxial loading and unloading conditions. The effect of the damage variable on the damage condition under uniaxial loading and

unloading conditions was also tested and verified. Using the test results, a correlative damage model for sandstone under loading and unloading conditions was determined, and the following conclusions were obtained:

(1) According to the development of rock fissures during the loading process, using the theory of fracture mechanics and the Archie formula, the mechanical properties and electrical properties of the rock were found to be related to each other via porosity. Through the theoretical model of resistivity and stress, the damage variable was defined to evaluate the degree of damage to the rock under loading and unloading conditions.

(2) By comparing the theoretical model and experimental test results, we found that the law of resistivity changed with stress in accordance with the stress-strain development law during uniaxial loading and unloading. This indicates that the rock damage variable D_ρ defined by the resistivity can describe the series of changes in the closure, initiation, and expansion of cracks in the rock sample at various stages of loading and unloading. At the same time, it also can be known that when the resistivity ratio drops close to 0.3, sandstone is likely to be destroyed, which is of certain significance in predicting the damage of bedrock under actual engineering.

(3) Through theoretical derivation and experimental research, a correlative damage model based on resistivity was established. The feasibility and accuracy of this model were verified using model parameter inversion and by comparing the theoretical and experimental curves. Thus, the damage evolution law of sandstone during uniaxial loading and unloading processes was clearly shown. This, in turn, provides a basis for evaluating the possible stress state of bedrock during loading and unloading processes in engineering scenarios.

The values of the correlative damage model parameters proposed in this paper still depend greatly on the experimental results. The correction factors (p, q, and r) will be changed under different conditions, which is because the correction factors are fitted according to the specific example and are the calibration parameters. Therefore, in order to assess more complex rock masses in engineering scenarios, the effects of the mechanical properties need to be studied further.

Therefore, in the next step, based on the results of this study, the physical meaning of the correction factors (ie., p, q, and r) in the correlative model will be proposed, and then the complete constitutive model of sandstone under cyclic loading and unloading conditions will be built.

Data Availability

The data used to support the findings of this study are available from the corresponding author upon request.

Conflicts of Interest

The authors declare that they have no conflicts of interest.

Acknowledgments

This research was funded by the Natural Science Foundation Project of China (Grant no. 51609027); the Chongqing Research Program of Basic Research and Frontier Technology (Grant number cstc2017jcyjBX0066); the Chongqing Research Program of Basic Research and Frontier Technology (Grant no. cstc2016jcyjA0016); Jiangxi Youth Science Fund Project (Grant no. 20171BAB216042); Chongqing Innovative Research Program for Graduatesthe (Grant no. CYB17127); Scientific and Technological Research Program of Chongqing Municipal Education Commission (Grant no. KJ1601005); and the Innovative Research Program for Graduates, Chongqing Jiaotong University (Grant no. 2019B0101). The authors are grateful to everyone without whose assistance the accomplishment of this thesis would have been impossible. Above all, the authors would like to thank their supervisor Mingjie Zhao for providing them with a particularly good research environment and platform. The authors are also grateful to Kui Wang for his patient guidance and constant encouragement during the writing of this thesis. Lastly, the authors would like to thank their other instructors for their valuable assistance.

References

[1] H. J. Su, H. W. Jing, H. H. Zhao, L. Y. Yu, and Y. C. Wang, "Strength degradation and anchoring behavior of rock mass in the fault fracture zone," *Environmental Earth Sciences*, vol. 76, no. 4, pp. 1–11, 2017.

[2] Q. Yin, H. W. Jing, H. J. Su, and H. H. Zhao, "Experimental study on mechanical properties and anchorage performances of rock mass in the fault fracture zone," *International Journal of Geomechanics*, vol. 18, no. 7, Article ID 04018067, 2018.

[3] M. N. Bagde and V. Petroš, "Fatigue properties of intact sandstone samples subjected to dynamic uniaxial cyclical loading," *International Journal of Rock Mechanics and Mining Sciences*, vol. 42, no. 2, pp. 237–250, 2005.

[4] M. N. Bagde and V. Petroš, "Fatigue and dynamic energy behaviour of rock subjected to cyclical loading," *International Journal of Rock Mechanics and Mining Sciences*, vol. 41, no. 1, pp. 200–209, 2009.

[5] M. J. Zhao, Z. C. Nie, K. Wang, P. Liu, and X. Zhang, "Nonlinear ultrasonic test of concrete cubes with induced crack," *Ultrasonics*, vol. 97, pp. 1–10, 2019.

[6] X. F. Liu, X. R. Wang, E. Y. Wang, Z. Liu, and X. Xu, "Study on ultrasonic response to mechanical structure of coal under loading and unloading condition," *Shock and Vibration*, vol. 2017, Article ID 7643451, 12 pages, 2017.

[7] X. Wang, E. Wang, and X. Liu, "Damage characterization of concrete under multi-step loading by integrated ultrasonic and acoustic emission techniques," *Construction and Building Materials*, vol. 221, pp. 678–690, 2019.

[8] X. Xu, B. Liu, S. Li, J. Song, M. Li, and J. Mei, "The electrical resistivity and acoustic emission response law and damage evolution of limestone in Brazilian split test," *Advances in Materials Science and Engineering*, vol. 2016, Article ID 8052972, 8 pages, 2016.

[9] S.-Q. Yang and H.-W. Jing, "Strength failure and crack coalescence behavior of brittle sandstone samples containing a single fissure under uniaxial compression," *International Journal of Fracture*, vol. 168, no. 2, pp. 227–250, 2011.

[10] W. F. Brance and A. S. Orange, "Electrical resistivity changes in saturated rock under stress," *Science*, vol. 153, no. 3743, pp. 1525-1526, 1966.

[11] T. Masao, Y. Isao, and F. Yoshio, "Anomalous electrical resistivity of almost dry marble and granite under axial compression," *Journal of Physics of the Earth*, vol. 41, no. 6, pp. 337–346, 1993.

[12] G. Chen and Y. Lin, "Stress-strain-electrical resistance effects and associated state equations for uniaxial rock compression," *International Journal of Rock Mechanics and Mining Sciences*, vol. 41, no. 2, pp. 223–236, 2004.

[13] C. Lü and Q. Sun, "Electrical resistivity evolution and brittle failure of sandstone after exposure to different temperatures," *Rock Mechanics and Rock Engineering*, vol. 51, no. 2, pp. 639–645, 2018.

[14] W. Zhang, Q. Sun, S. Zhu, and S. Hao, "The effect of thermal damage on the electrical resistivity of sandstone," *Journal of Geophysics and Engineering*, vol. 14, no. 2, pp. 255–261, 2017.

[15] S. Kahraman and T. Yeken, "Electrical resistivity measurement to predict uniaxial compressive and tensile strength of igneous rocks," *Bulletin of Materials Science*, vol. 33, no. 6, pp. 731–735, 2010.

[16] T. Han, A. I. Best, J. Sothcott, and L. M. MacGregor, "Pressure effects on the joint elastic-electrical properties of reservoir sandstones," *Geophysical Prospecting*, vol. 59, no. 3, pp. 506–517, 2011.

[17] A. P. Garcia, A. Jagadisan, A. Rostami, and Z. Heidari, "A new resistivity-based model for improved hydrocarbon saturation assessment in clay-rich formations using quantitative clay network geometry and rock fabric," in *Proceedings of The SPWLA 58th Annual Logging Symposium*, Society of Petrophysicists and Well-log Analysts, Oklahoma City, OK, USA, 2017.

[18] Y.-H. Wang, Y.-F. Liu, and H.-T. Ma, "Changing regularity of rock damage variable and resistivity under loading condition," *Safety Science*, vol. 50, no. 4, pp. 718–722, 2012.

[19] K. B. Yang, J. F. Wang, F. Q. Ma, H. Y. Tang, and X. F. Pan, "Analysis and countermeasures about applicable conditions of Archie's Formula," *Oil & Gas Exploration and Development*, vol. 36, no. 2, pp. 58–63, 2018, in Chinese.

[20] G. E. Archie, "The electrical resistivity log as an aid in determining some reservoir characteristics," *Transactions of the AIME*, vol. 146, no. 1, pp. 54–62, 1942.

[21] Y. H. Dai, *CT Testing Analysis and Constitutive Model Study of Unsaturated Slates*, Wuhan Institute of Rock & Soil Mechanics the Chinese Academy of Sciences, Wuhan, China, 2006, in Chinese.

[22] R. E. Goodman and W. Boyle, "Non-linear analysis for calculating the support of a rock block with dilatant joint faces," *Computers and Geotechnics*, vol. 3, no. 1, p. 62, 1987.

[23] T. H. Huang, C. S. Chang, and C. Y. Chao, "Experimental and mathematical modeling for fracture of rock joint with regular asperities," *Engineering Fracture Mechanics*, vol. 69, no. 17, pp. 1977–1996, 2002.

[24] M. J. Zhao, *Acoustic Characteristics of Loaded Rock Concrete and its Application*, Beijing Science Press, Beijing, China, 2009, in Chinese.

[25] R. J. O'Connell and B. Budiansky, "Seismic velocities in dry and saturated cracked solids," *Journal of Geophysical Research*, vol. 79, no. 35, pp. 5412–5426, 1974.

[26] J. Yang and X. Heping, "A variable condition of the damage description based on hypothesis of strain equivalence," *Chinese Journal of Applied Mechanics*, vol. 15, pp. 43–49, 1998, in Chinese.

[27] Y. Liu, F. Dai, P. Fan, N. Xu, and L. Dong, "Experimental investigation of the influence of joint geometric configurations on the mechanical properties of intermittent jointed rock models under cyclic uniaxial compression," *Rock Mechanics and Rock Engineering*, vol. 50, no. 6, pp. 1453–1471, 2017.

[28] Y. Liu, F. Dai, L. Dong, N. Xu, and P. Feng, "Experimental investigation on the fatigue mechanical properties of intermittently jointed rock models under cyclic uniaxial compression with different loading parameters," *Rock Mechanics and Rock Engineering*, vol. 51, no. 1, pp. 47–68, 2018.

[29] Y. Liu and F. Dai, "A damage constitutive model for intermittent jointed rocks under cyclic uniaxial compression," *International Journal of Rock Mechanics and Mining Sciences*, vol. 103, pp. 289–301, 2018.

[30] X. S. Liu, J. G. Ning, Y. L. Tan, and Q. H. Gu, "Damage constitutive model based on energy dissipation for intact rock subjected to cyclic loading," *International Journal of Rock Mechanics and Mining Sciences*, vol. 85, pp. 27–32, 2016.